

# Micellization and Gelation of Triblock Copolymers of Ethylene Oxide and Styrene Oxide in Aqueous Solution

Zhuo Yang,<sup>†</sup> Michael Crothers,<sup>‡</sup> Nágila M. P. S. Ricardo,<sup>§</sup> Chiraphon Chaibundit,<sup>||</sup> Pablo Taboada,<sup>⊥</sup> Victor Mosquera,<sup>⊥</sup> Antonis Kalarakis,<sup>∞</sup> Vassiliki Havredaki,<sup>∞</sup> Luigi Martini,<sup>Δ</sup> Christopher Valder,<sup>Δ</sup> John H. Collett,<sup>‡</sup> David Attwood,<sup>\*,‡</sup> Frank Heatley,<sup>†</sup> and Colin Booth<sup>†</sup>

Department of Chemistry and School of Pharmacy and Pharmaceutical Sciences, University of Manchester, Manchester M13 9PL, United Kingdom, Department of Organic and Inorganic Chemistry, Federal University of Ceará, CX 12200 Fortaleza, Brazil, Polymer Science Program, Faculty of Science, Prince of Songkla University, Songkhla 90112, Thailand, Department of Physics of Condensed Matter, University of Santiago de Compostela, E-15706 Santiago de Compostela, Spain, Department of Chemistry, Physical Chemistry Laboratory, National and Kapodistrian University of Athens, Panepistimiopolis, 157 71 Athens, Greece, and GlaxoSmithKline, New Frontiers Science Park (South), Harlow, Essex CM19 5AW, United Kingdom

Received August 27, 2002. In Final Form: November 22, 2002

Nine triblock copolymers of ethylene oxide and styrene oxide (type  $E_mS_nE_m$ , E = oxyethylene, S = oxyphenylethylene,  $n$  and  $m$  = number-average block lengths) were prepared by sequential oxyanionic polymerization. Surface tensiometry was used to determine critical micelle concentrations (cmc's) and standard enthalpies of micellization, and isothermal titration calorimetry was used to confirm the enthalpy of micellization. Light scattering was used to determine micellar association numbers and hydrodynamic radii. Phase diagrams defining regions of hard and soft gel were determined by tube inversion and Couette rheometry. Comparison is made with reported results for diblock copolymers of ethylene oxide and styrene oxide and, so far as possible, with results for triblock copolymers of ethylene oxide and styrene. Compilation of values of the cmc for three series of triblock copoly(oxyalkylene)s,  $E_mS_nE_m$ ,  $E_mB_nE_m$  (B = oxybutylene), and  $E_mP_nE_m$  (P = oxypropylene), reveals a discontinuity in the block length dependence of  $\log(\text{cmc})$  at  $S_6$  and  $B_{12}$ .

## 1. Introduction

Water-soluble block copolymers with narrow block length distributions can be readily prepared by sequential oxyanionic polymerization from ethylene oxide and a second epoxide.<sup>1,2</sup> The combination of a hydrophilic poly(oxyethylene) block with a second hydrophobic block confers interesting and useful properties of surface activity and micellization in dilute solution and of gelation of concentrated solutions. Variation of the hydrophobic block, the block length, and the block architecture allows close control of properties. Commercially available block copolymers of ethylene oxide with propylene oxide or 1,2-butylene oxide have been available for some time and have provided materials for academic research, and the range has been significantly extended by laboratory synthesis.<sup>1–3</sup> The significant factor distinguishing these

two types of copolymer is the hydrophobicity of the chain unit. Denoting an oxypropylene unit [ $\text{OCH}_2\text{CH}(\text{CH}_3)$ ] by P and an oxybutylene unit [ $\text{OCH}_2\text{CH}(\text{C}_2\text{H}_5)$ ] by B, their hydrophobicities based on the molar critical micelle concentrations (cmc) of diblock copolymers are in ratio P:B = 1:6.<sup>3</sup> As a consequence, copolymers with short B blocks have similar association properties to copolymers with long P blocks, giving considerable flexibility in the design of materials for end use.

This range of hydrophobicity can be extended while the simplicity of the chemistry is maintained by use of styrene oxide. Materials of this type have recently been marketed by Goldschmidt AG, Essen. The chain unit in the copolymer (denoted S) is oxyphenylethylene [ $\text{OCH}_2\text{CH}(\text{C}_6\text{H}_5)$ ], and the ratio of hydrophobicities is B:S = 1:2, again judged by the values of the cmc for diblock copolymers in molar units.<sup>3</sup> In fact, the hydrophobicity of an S unit is the same as that of the phenylethylene unit (here denoted St) of poly(styrene). However, the preparation of S-containing copolymers is entirely by oxyanion chemistry and does not require part-synthesis by carbanion or atom transfer chemistry. Moreover, the lower glass transition temperature of poly(styrene oxide) ( $T_g \approx 40^\circ\text{C}$ )<sup>4</sup> compared to poly(styrene) ( $T_g \approx 100^\circ\text{C}$ ) means that effects caused by immobility of blocks in the micelle core (the cores of St blocks have been referred to as "frozen")<sup>5</sup> are unimportant in micellar solutions of E/S

<sup>†</sup> Department of Chemistry, University of Manchester.

<sup>‡</sup> School of Pharmacy and Pharmaceutical Sciences, University of Manchester.

<sup>§</sup> Federal University of Ceará.

<sup>||</sup> Prince of Songkla University.

<sup>⊥</sup> University of Santiago de Compostela.

<sup>∞</sup> National and Kapodistrian University of Athens.

<sup>Δ</sup> GlaxoSmithKline.

(1) *Nonionic Surfactants, Poly(oxyalkylene) Block Copolymers, Surfactant Science Series*; Nace, V. M., Ed.; Marcel Dekker: New York, 1996; Vol. 60.

(2) *Amphiphilic Block Copolymers: Self-assembly and Applications*; Alexandridis, P., Lindman, B., Eds.; Elsevier Science: Amsterdam, 2000.

(3) Booth, C.; Attwood, D. *Macromol. Rapid Commun.* **2000**, *21*, 501.

(4) Allen, G.; Booth, C.; Hurst, S. J.; Price, C.; Vernon, F.; Warren, R. F. *Polymer* **1967**, *8*, 406.

copolymers ( $E = \text{oxyethylene, OCH}_2\text{CH}_2$ ). For example, we have already shown that solubilization of an aromatic drug (griseofulvin) is possible in the mobile cores of E/S copolymer micelles at room temperature. Indeed, no doubt because of the aromaticity of the micelle core, the extent of solubilization of griseofulvin at that temperature is enhanced compared with E/P and E/B counterparts.<sup>6</sup>

Our recent work on the micellization and micelle properties of E/S copolymers has involved only diblock copolymers.<sup>7–10</sup> Here we report the preparation and the association properties in aqueous solution of nine triblock copolymers,  $E_mS_nE_m$  with  $n$  in the range 5–19 and  $m$  in the range 65–142, the subscripts denoting number-average block lengths. The association properties of several triblock copolymers of ethylene oxide and styrene [type  $E_mSt_nE_m$ ,  $St = \text{phenylethylene, CH}_2\text{CH(C}_6\text{H}_5\text{)}$ ] in aqueous solution have been reported and provide data for comparison with those of the new  $E_mS_nE_m$  copolymers.<sup>11–13</sup> However, a severe limitation is that the great majority of the St blocks of the copolymers studied are much longer than the S blocks used in our work.

## 2. Experimental Section

**2.1. Copolymers.** The triblock copolymers were prepared by sequential anionic polymerization of styrene oxide followed by ethylene oxide. The general method has been described previously.<sup>7,8</sup> High vacuum and ampule techniques were used to eliminate unwanted moisture. Initiation of the difunctional precursor was either by potassium hydroxide and water or by 1,2-butanediol partly in the form of its potassium salt. Butane-1,2-diol provided a more convenient initiation system and, as the hydrophobicity of a B unit is known to be half that of an S unit,<sup>3</sup> the formula could be readily adjusted to take account of the extra unit in the central block. In each case the mole ratio OH/OK  $\approx$  9, this being chosen to achieve a suitable polymerization rate. The monomers were distilled and dried immediately before use. Styrene oxide was added to the ampule by syringe, and for the second stage of polymerization, ethylene oxide was distilled through the vacuum line. The polymerization of styrene oxide at 85 °C was slow, taking as long as 8 weeks. The polymerization of ethylene oxide was relatively fast, reaching completion in 3 weeks or less.

The precursor, sampled at the end of stage one, and the final copolymer were characterized by gel permeation chromatography (GPC), matrix-assisted laser-desorption ionization (MALDI) mass spectroscopy, and <sup>13</sup>C NMR spectroscopy. Depending on sample, the eluent for GPC was either tetrahydrofuran at 25 °C or *N,N*-dimethylacetamide at 60 °C. Calibration was with poly(oxyethylene) or poly(styrene) samples of known molar mass, as appropriate. Analysis of the GPC curves gave an estimate of the

**Table 1. Molecular Characteristics of the ESE Block Copolymers<sup>a</sup>**

copolymer	$M_n/\text{g mol}^{-1}$	wt % E	$M_w/M_n$	$M_w^b/\text{g mol}^{-1}$
E <sub>76</sub> S <sub>5</sub> E <sub>76</sub> <sup>c</sup>	7350	91	1.06	7790
E <sub>82</sub> S <sub>8</sub> E <sub>82</sub> <sup>c</sup>	8150	89	1.07	8720
E <sub>82</sub> S <sub>9</sub> E <sub>82</sub> <sup>c</sup>	8340	87	1.06	8840
E <sub>69</sub> S <sub>8</sub> E <sub>69</sub>	7030	89	1.05	7380
E <sub>65</sub> S <sub>11</sub> E <sub>65</sub>	7040	81	1.05	7390
E <sub>66</sub> S <sub>13</sub> E <sub>66</sub>	7370	79	1.04	7660
E <sub>67</sub> S <sub>15</sub> E <sub>67</sub>	7700	77	1.04	8100
E <sub>112</sub> S <sub>9</sub> E <sub>112</sub>	11000	90	1.08	11900
E <sub>142</sub> S <sub>19</sub> E <sub>142</sub>	14800	84	1.09	16100

<sup>a</sup> Estimated uncertainties:  $M_n$ ,  $\pm 3\%$ ; wt % E,  $\pm 1\%$ ;  $M_w/M_n$ ,  $\pm 0.01$ .

<sup>b</sup>  $M_w$  was calculated from  $M_n$  and  $M_w/M_n$ . <sup>c</sup> Copolymers initiated using butane-1,2-diol.

width of the molar mass distribution of the samples in the form of the ratio of mass-average to number-average molar mass ( $M_w/M_n$ ). NMR spectra of samples (10 wt % in CDCl<sub>3</sub>) were recorded by means of a Varian Unity 500 spectrometer operated at 125.5 MHz. Peak assignments were taken from previous work by Heatley et al.<sup>14</sup> The integrals of resonances from backbone and end group carbons of the precursor S block were used to determine S block length, and the average composition of the copolymer then gave the E-block length and hence the molecular formula. Allowance was made for the different nuclear Overhauser enhancements of E and S units, i.e. E/S = 1.1. The triblock architecture and the purity of the copolymers were confirmed by comparison of resonances from the carbons of end and junction groups. The values of  $M_n$  obtained by MALDI mass spectroscopy (Micromass TOF Spec2E) were in good agreement with those from NMR. The molecular characteristics of the copolymers are summarized in Table 1.

**2.2. Surface Tension.** Surface tensions ( $\gamma$ ) of dilute aqueous solutions were measured at four temperatures in the range 25–50 °C using temperature-controlled ( $\pm 0.2$  °C) surface tensiometers equipped with either a platinum plate or a platinum ring. A new solution was first equilibrated at the lowest temperature for 24 h and then  $\gamma$  was measured every 1 h until consistent readings were obtained. Thereafter the temperature was raised and the procedure repeated. Before a new solution was used, the probe was washed successively with dilute acid and water. The accuracy of measurement was checked by frequent determination of the surface tension of pure water.

**2.3. Isothermal Titration Calorimetry.** Heats of dilution were measured using a VP-ITC titration microcalorimeter from MicroCal Inc., Northampton, MA. Small aliquots (5–10 mm<sup>3</sup>) of stock solution of copolymer at a concentration well above the cmc were injected into a known volume of water held in the cell of the calorimeter, initially to produce a solution below the cmc. Repeated additions of the stock solution gave the enthalpy of dilution ( $\Delta_{\text{dil}}H$ ) as a function of copolymer concentration. These data were analyzed using the method suggested by Klijn et al.<sup>15</sup> and investigated by others<sup>16</sup> to obtain the enthalpy of demicellization ( $\Delta_{\text{demic}}H$ ) and the cmc, the latter being identified with the start of the micellization process.

**2.4. Light Scattering.** All glassware was washed with condensing acetone vapor before use. Solutions were clarified by filtering through Millipore Millex filters (Triton free, 0.22- $\mu\text{m}$  porosity) directly into the cleaned scattering cell. Static light scattering (SLS) intensities were measured for solutions at temperatures in the range 25–50 °C by means of a Brookhaven BI200S instrument with vertically polarized incident light of wavelength  $\lambda = 488$  nm supplied by an argon ion laser (Coherent Innova 90) operated at 500 mW or less. The intensity scale was calibrated against scattering from benzene. Dynamic light scattering (DLS) measurements were made under similar conditions by means of the Brookhaven BI200S combined with a Brookhaven BI9000AT digital correlator. Experiment duration

(14) Heatley, F.; Yu, G.-E.; Draper, M. D.; Booth, C. *Eur. Polym. J.* **1991**, *27*, 471.

(15) Klijn, J. E.; Kevalam, J.; Engberts, J. B. F. N. *J. Colloid Interface Sci.* **2000**, *226*, 76.

(16) Raju, B. B.; Winnick, F. M.; Morishima, Y. *Langmuir* **2001**, *17*, 4416.

(5) (a) Hurtez, G.; Dumas, P.; Riess, G. *Polym. Bull.* **1998**, *40*, 203. (b) Jada, A.; Hurtez, G.; Siffert, B.; Riess, G. *Macromol. Chem. Phys.* **1996**, *197*, 3697.

(6) Rekasas, C. J.; Mai, S.-M.; Crothers, M.; Quinn, M.; Collett, J. H.; Attwood, D.; Heatley, F.; Martini, L.; Booth, C. *Phys. Chem. Chem. Phys.* **2001**, *3*, 4769.

(7) Mai, S.-M.; Booth, C.; Kellarakis, A.; Havredaki, V.; Ryan, A. J. *Langmuir* **2000**, *16*, 1681.

(8) Kellarakis, A.; Havredaki, V.; Rekasas, C. J.; Mai, S.-M.; Attwood, D.; Booth, C.; Ryan, A. J.; Hamley, I. W.; Martini, L. *Macromol. Chem. Phys.* **2001**, *202*, 1345.

(9) Kellarakis, A.; Havredaki, V.; Rekasas, C. J.; Booth, C. *Phys. Chem. Chem. Phys.* **2001**, *3*, 5550.

(10) Crothers, M.; Attwood, D.; Collett, J. H.; Yang, Z.; Booth, C.; Taboada, P.; Mosquera, V.; Ricardo, N. M. P. S.; Martini, L. *Langmuir* **2002**, *18*, 8685.

(11) Bahadur, P.; Sastry, N. V. *Eur. Polym. J.* **1988**, *24*, 285.

(12) (a) Xu, R.; Winnick, M. A.; Hallett, F. R.; Riess, G.; Croucher, M. D. *Macromolecules* **1991**, *24*, 87. (b) Wilhelm, M.; Zhao, C.-L.; Wang, Y.; Xu, R.; Winnick, M. A.; Mura, J.-L.; Riess, G.; Croucher, M. D. *Macromolecules* **1991**, *24*, 1033. (c) Xu, R.; Winnick, M. A.; Riess, G.; Chu, B.; Croucher, M. D. *Macromolecules* **1992**, *25*, 644. (d) Xu, R.; Hu, Y.; Winnick, M. A.; Riess, G.; Croucher, M. D. *J. Chromatogr.* **1991**, *547*, 434. (e) Zhao, C.-L.; Winnick, M. A.; Riess, G.; Croucher, M. D. *Langmuir* **1990**, *6*, 514.

(13) Jada, A.; Siffert, B.; Riess, G. *Colloids Surf. A* **1993**, *75*, 203.

was in the range 10–20 min and each experiment was repeated two or more times. Measurements of scattered light were normally made at  $\theta = 90^\circ$  to the incident beam, but some measurements were made at other angles to check that the angular dependence of intensity was unimportant.

The correlation functions from DLS were analyzed by the constrained regularized CONTIN method to obtain distributions of decay rates ( $\Gamma$ ).<sup>17</sup> The decay rate distributions gave distributions of the apparent diffusion coefficient [ $D_{\text{app}} = \Gamma/q^2$ ,  $q = (4\pi n_s/\lambda) \sin(\theta/2)$ ,  $n_s$  = refractive index of water] and hence of apparent hydrodynamic radius ( $r_{\text{h,app}}$ , radius of hydrodynamically equivalent hard sphere corresponding to  $D_{\text{app}}$ ) through the Stokes–Einstein equation

$$r_{\text{h,app}} = kT/(6\pi\eta D_{\text{app}}) \quad (1)$$

where  $k$  is the Boltzmann constant and  $\eta$  is the viscosity of water at temperature  $T$ .

The basis for the analysis of SLS was the Debye equation

$$K^* d(I - I_s) = 1/M_w + 2A_2c + \dots \quad (2)$$

where  $I$  is intensity of light scattering from solution relative to that from benzene,  $I_s$  is the corresponding quantity for the solvent,  $c$  is the concentration (in  $\text{g dm}^{-3}$ ),  $M_w$  is the mass-average molar mass of the solute,  $A_2$  is the second virial coefficient (higher coefficients being neglected), and  $K^*$  is the appropriate optical constant that includes the specific refractive index increment,  $\nu = dn/dc$ .

Refractive indices of block copolymer solutions with concentrations in the range 0–10 wt % were measured by means of a precision Abbé refractometer (Bellingham-Stanley Ltd.). The scale was checked using poly(oxyethylene). Determination of the specific refractive index increment at 30 °C for a range of block copolymers of ethylene oxide and styrene oxide, including those previously described,<sup>5</sup> gave

$$\nu/(\text{cm}^3 \text{g}^{-1}) = 0.134 + 0.067w_S \quad (3)$$

where  $w_S$  is the weight fraction of S. The temperature derivative of  $\nu$  was taken to be that established previously<sup>18</sup> for other poly(oxyethylene)-containing water-soluble block copolymers, i.e.  $-2.3 \times 10^{-4} \text{ cm}^3 \text{ g}^{-1} \text{ K}^{-1}$ .

**2.5. Rheometry.** Solutions were prepared by weighing copolymer and water into small tubes and mixing, if possible, in the mobile state before being stored for a day or more at low temperature ( $T \approx 5^\circ\text{C}$ ). Otherwise, the mixture was allowed to mix by diffusion over a period of days at 5 °C.

In tube inversion experiments, the tubes (internal diameter 10 mm containing 0.5 g of solution) were heated (or cooled) at ca.  $0.5^\circ\text{C min}^{-1}$  in a water bath. With the temperature held steady, the change from a mobile to an immobile system (or vice-versa) was determined by inverting the tube.

Rheological properties of the solutions were determined using a Bohlin CS50 rheometer with water bath temperature control. Couette geometry (bob, 24.5 mm diameter, 27 mm height; cup, 26.5 mm diameter, 29 mm height) was used, with 2.5 mL of sample being added to the cup in the mobile state. A solvent trap maintained a water-saturated atmosphere around the cell, and evaporation was not significant for the temperatures and time scales investigated. Storage and loss moduli were recorded across the temperature range with the instrument in oscillatory-shear mode at a frequency of 1 Hz. The strain amplitude was maintained at a low value ( $<0.6\%$ ) by means of the autostress facility in the Bohlin software. This ensured that moduli were essentially independent of strain. The solutions were heated at ca.  $1^\circ\text{C min}^{-1}$  in the range 5–85 °C.

### 3. Results and Discussion

**3.1. Clouding.** Solutions were observed during the tube inversion tests (concentration range 0 to 80 wt %) and

**Table 2. Critical Micelle Concentrations, Surface Tensions, and Enthalpies of Micellization for ESE Block Copolymers in Aqueous Solutions<sup>a</sup>**

copolymer	method	$T/^\circ\text{C}$	cmc/ $\text{g dm}^{-3}$	$\gamma_{\text{cmc}}/m\text{N m}^{-1}$	$\Delta_{\text{mic}}H_{\text{app}}^{\circ}/kJ \text{ mol}^{-1}$	
E <sub>82</sub> S <sub>8</sub> E <sub>82</sub>	ST	20	0.51	56.8	$40 \pm 5$	
		30	0.26	54.5		
		40	0.20	52.8		
		50	0.10	50.8		
E <sub>82</sub> S <sub>9</sub> E <sub>82</sub>	ST	30	0.11	53.6	$8.0 \pm 2$	
		E <sub>65</sub> S <sub>11</sub> E <sub>65</sub>	25	0.12		51.5
			30	0.095		50.5
			40	0.095		49.1
E <sub>66</sub> S <sub>13</sub> E <sub>66</sub>	ST	50	0.085	47.5	$4.4 \pm 1$	
		25	0.051	48.6		
		30	0.050	47.7		
		40	0.048	46.3		
E <sub>67</sub> S <sub>15</sub> E <sub>67</sub>	ST	50	0.045	45.0	$4.1 \pm 1$	
		25	0.026	46.8		
		30	0.025	45.7		
		40	0.024	44.2		
E <sub>69</sub> S <sub>8</sub> E <sub>69</sub>	ITC	50	0.022	42.6	$10 \pm 5^b$	
		30	0.11			
E <sub>112</sub> S <sub>9</sub> E <sub>112</sub>	ITC	30	0.14		$27 \pm 10^b$	

<sup>a</sup> Estimated uncertainties: cmc to  $\pm 10\%$ ,  $\gamma_{\text{cmc}}$  to  $\pm 1\%$ . <sup>b</sup> Calorimetric enthalpy of micellization.

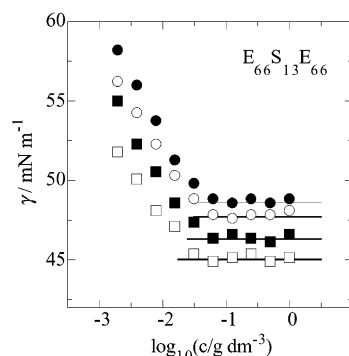


**Figure 1.** Surface tension ( $\gamma$ ) versus logarithm of concentration for aqueous solutions of block copolymer E<sub>66</sub>S<sub>13</sub>E<sub>66</sub> at (●) 25, (○) 30, (■) 40, and (□) 50 °C.

remained clear to the eye throughout the temperature range investigated (10–95 °C).

**3.2. Critical Micelle Concentration.** The surface tensions of solutions of four samples were investigated, as set out in Table 2. As an example, plots of surface tension against  $\log(\text{concentration})$  obtained for copolymer E<sub>66</sub>S<sub>13</sub>E<sub>66</sub> are shown in Figure 1. The concentration at which the surface tension reached a steady value served to define the cmc. Representative values of the cmc and of the surface tension at the cmc are listed in Table 2.

Comparison of values of the cmc for the present triblock copolymers with those reported for diblock E/S copolymers<sup>7,9,10</sup> is made in Figure 2. The plot is of  $\log(\text{cmc})$  against S-block length, with the cmc in units of  $\text{mol dm}^{-3}$ . As described below (eq 6),  $\log(\text{cmc}/\text{mol dm}^{-3})$  is approximately proportional to the Gibbs energy of micellization. It is known that the values of the cmc in molar units of block copolymers of this type are only weakly dependent on E-block length.<sup>3,19</sup> In fact, the E-block lengths of the diblock comparators (E<sub>45</sub>–E<sub>60</sub>) are similar to those of the present copolymers. As seen in Figure 2, compared at equivalent S-block length, the values of the cmc for the triblock copolymers (open circles) lie roughly 1 order of magnitude higher than those of the E<sub>m</sub>S<sub>n</sub> diblocks (filled circles).

(17) Provencher, S. W. *Makromol. Chem.* **1979**, *180*, 201.

(18) Bedells, A. D.; Arafeh, R. M.; Yang, Z.; Attwood, D.; Heatley, F.; Padgett, J. C.; Price, C.; Booth, C. *J. Chem. Soc., Faraday Trans.* **1993**, *89*, 1235.

(19) Kellarakis, A.; Yang, Z.; Pousia, E.; Nixon, S. K.; Price, C.; Booth, C.; Hamley, I. W.; Castelletto, V.; Fundin, J. *Langmuir* **2001**, *17*, 8085.

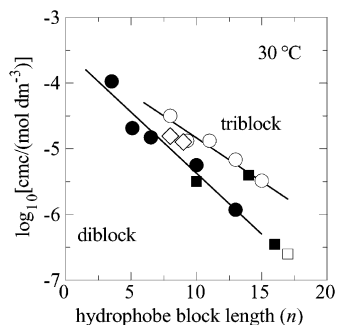


**Figure 2.** Logarithm of cmc (in mol dm<sup>-3</sup>) versus hydrophobe block length ( $n$ ) for aqueous solutions at 30 °C of (○, ◇) triblock E<sub>m</sub>S<sub>n</sub>E<sub>m</sub> copolymers compared with results for (●) diblock E<sub>m</sub>S<sub>n</sub> and S<sub>n</sub>E<sub>m</sub> copolymers taken from refs 7, 9, and 10. The data points denoted ◇ are from ITC. Comparison is made with published results for (■) diblock St<sub>n</sub>E<sub>m</sub> (refs 12b, 20, 21) and (□) triblock E<sub>m</sub>St<sub>n</sub>E<sub>m</sub> (ref 12b) copolymers.

Similar results have been reported for diblock and triblock E/B and E/P copolymers.<sup>3</sup>

Comparison with reported results for diblock and triblock copolymers of ethylene oxide and styrene with St blocks in the range of interest is also made in Figure 2. As discussed previously,<sup>3,10</sup> on balance the available data for the diblock copolymers (St<sub>10</sub>E<sub>68</sub>, St<sub>14</sub>E<sub>160</sub>, St<sub>16</sub>E<sub>155</sub>)<sup>12b,20,21</sup> favor a similar hydrophobicity for S and St units. The one reported result for EStE copolymers in the required range ( $n < 20$ ) is for triblock copolymer E<sub>205</sub>St<sub>17</sub>E<sub>205</sub>.<sup>12b</sup> As can be seen in Figure 2, this result is out of line, not only with the results for the ESE triblocks, but also with those for the StE diblocks since, other things being equal, higher values of the cmc are expected for triblock copolymers compared with diblocks with the same hydrophobe block length.<sup>3</sup> In fact, the values reported<sup>12b</sup> for EStE copolymers with longer St blocks, e.g. log(cmc/mol dm<sup>-3</sup>) = -6.86 for copolymer E<sub>164</sub>S<sub>35</sub>E<sub>164</sub>, lie above the extrapolation of the line for the ESE triblocks.

**3.2.1. Thermodynamics of Micellization.** For closed association to micelles with a narrow distribution of association number ( $N$ ), the equilibrium between copolymer molecules (A) and micelles (A<sub>N</sub>) can be written (concentration in mol dm<sup>-3</sup>) as

$$K_c = [A_N]_{\text{eq}}^{1/N} / [A]_{\text{eq}} \quad (4)$$

If the association number is sufficiently large, then the equilibrium constant is well-approximated by

$$K_c = 1/[A]_{\text{eq}} \quad (5)$$

where  $[A]_{\text{eq}}$  is the cmc at the appropriate temperature. Accordingly, without further approximation, for the forward reaction in the equilibrium the standard Gibbs energy of micellization is

$$\Delta_{\text{mic}}G^\circ = -RT \ln K_c = RT \ln(\text{cmc}) \quad (6)$$

and the standard enthalpy of micellization is

$$\Delta_{\text{mic}}H^\circ = -R d[\ln(K_c)]/d(1/T) = R d[\ln(\text{cmc})]/d(1/T) \quad (7)$$

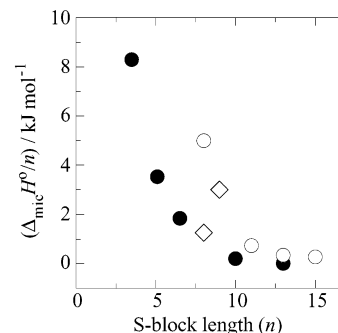


**Figure 3.** Standard enthalpy of micellization per S unit ( $\Delta_{\text{mic}}H^\circ/n$ ) for aqueous solutions of (○, ◇) triblock ESE copolymers (present work) compared with results for (●) diblock copolymers taken from refs 7, 9, and 10. The values of  $\Delta_{\text{mic}}H^\circ$  from ITC are denoted ◇.

The process referred to is that of copolymer chains in their standard state of ideally dilute solution at unit concentration (1 mol dm<sup>-3</sup>) going to copolymer chains in the micellar state. For eq 7 to apply to equilibrium 4 it is necessary that eq 6 is a fair approximation at all temperatures. In fact, the mass-average association numbers ( $N_w$ ) of the triblock copolymers investigated by surface tensiometry at several temperatures range from 11 to 30 (see Section 3.3), and in relation to the equilibrium constant, the values of the standard enthalpy of micellization obtained are best described as apparent ( $\Delta_{\text{mic}}H^\circ_{\text{app}}$ ; see Table 2). Of course, the quoted values of  $\Delta_{\text{mic}}H^\circ_{\text{app}}$  do correctly describe the temperature dependence of the cmc.

As seen in Table 2, the values obtained for  $\Delta_{\text{mic}}H^\circ_{\text{app}}$  are in the range 4–40 kJ mol<sup>-1</sup>. Isothermal titration calorimetry at 30 °C confirmed similarly low values of the calorimetric enthalpy for copolymers E<sub>69</sub>S<sub>8</sub>E<sub>69</sub> and E<sub>112</sub>S<sub>9</sub>E<sub>112</sub>.

Figure 3 shows the standard enthalpy of micellization per S unit ( $\Delta_{\text{mic}}H^\circ/n$ ) plotted against  $n$ . The enthalpy of micellization from ITC for copolymers E<sub>112</sub>S<sub>9</sub>E<sub>112</sub> and E<sub>69</sub>S<sub>8</sub>E<sub>69</sub> are included. Comparison is made with values for diblock ES copolymers.<sup>7,9,10</sup> As discussed in detail previously,<sup>9</sup> the very low standard enthalpy change per S unit found for the copolymers with the longer S blocks is attributable to those blocks being tightly coiled in the dispersed molecular state, so that the interaction of an S unit with water is much reduced in comparison with the interaction enthalpies of the units of the shorter blocks, which are more extended in the molecular state. Presumably, the generally higher values of  $\Delta_{\text{mic}}H^\circ/n$  found for the triblock copolymers reflect a greater extension of their S blocks resulting from the two E blocks.

**3.2.2. Comparison with Results for EBE and EPE Copolymers.** In Figure 4, results for the triblock ESE copolymers (taken from Table 2) are compared with the published values for EBE and EPE copolymers summarized in refs 3 and 22. To allow for differences in hydrophobicity, values of log(cmc) are plotted against  $x = n$  for ESE copolymers,  $x = n/2$  for EBE copolymers, and  $x = n/10$  for EPE copolymers. For the EPE copolymers, division by 10 rather than 12 (as found for diblock copolymers; see Section 1) is preferred, as this brings the data points for EBE and EPE copolymers into close coincidence (see Figure 4). The effect of E-block length on the cmc in molar units is small compared to that of the hydrophobic block length and is unimportant on a log scale. There is a marked change in slope at  $x = 6$ , equivalent to

(20) Dewhurst, P. F.; Lovell, M. R.; Jones, J. L.; Richards, R. W.; Webster, J. R. P. *Macromolecules* **1998**, *31*, 7851.

(21) Mortensen, K.; Brown, W.; Almdal, K.; Alami, E.; Jada, A. *Langmuir* **1997**, *13*, 3635.

(22) Chu, B.; Zhou, Z.-K. In *Nonionic Surfactants, Poly(oxyalkylene) Block Copolymers, Surfactant Science Series*; Nace, V. M. Ed.; Marcel Dekker: New York, 1996; Vol. 60, Chapter 3.

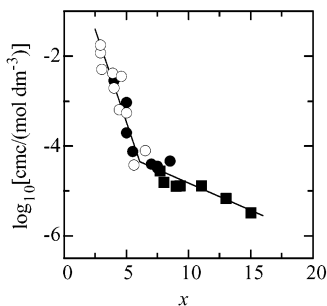


**Figure 4.** Dependence of cmc on hydrophobe block length for triblock copolymers in aqueous solutions at 30 °C: (■) ESE copolymers from Figure 2 ( $x = \text{S-block length} = n$ ), (●) EBE copolymers from ref 3 ( $x = \text{B-block half-length} = n/2$ ), (○) EPE copolymers from refs 3 and 22 ( $x = \text{P-block tenth-length} = n/10$ ).

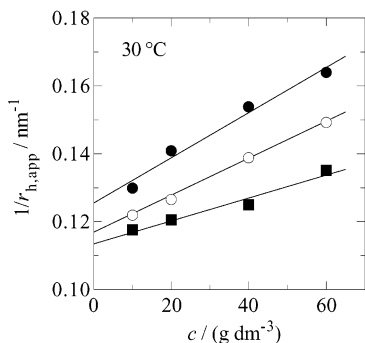


**Figure 5.** Concentration dependence of reciprocal apparent hydrodynamic radius for aqueous micellar solutions at 30 °C: (●)  $E_{65}S_{11}E_{65}$ , (○)  $E_{66}S_{13}E_{66}$ , (■)  $E_{67}S_{15}E_{67}$ .

$B_{12}$ . The slope of the line through the data points at high  $x$  is one-sixth that at low  $x$ , implying, through eq 6, a similar factor in the block length dependence of  $\Delta_{\text{mic}}^{\circ} G_{\text{app}}^{\circ}$ . A similar change in slope was found at  $x = 5$  for ES and EB diblock copolymers when compared in this way.<sup>10</sup> As noted in Section 3.2.1, it is likely that the ESE copolymers have their hydrophobic blocks tightly coiled in their molecular state in aqueous solution, thus limiting their contact with water and reducing the hydrophobic effect. The same is true of EBE copolymers with blocks longer than  $B_{12}$ . However, the longest P block among the commercially available EPE copolymers is  $P_{65}$  (e.g. Pluronic F127) and the effect, if any, cannot be detected.

### 3.3. Association Number and Micelle Radius.

Usually light scattering measurements were made for solutions at 25, 30, 40, and 50 °C and at concentrations in the range 5–60 g dm<sup>-3</sup>. Under all conditions, the intensity fraction distributions of  $\log r_{h,\text{app}}$  obtained from DLS (not shown) comprised single narrow peaks, indicative of closed micellization. Plots of the reciprocal of the intensity average of  $r_{h,\text{app}}$  against concentration were linear; see Figure 5 for examples. The intercepts of these plots at  $c = 0$  gave values of  $r_h$ . As shown by the representative values listed in Table 3, within experimental error temperature had very little effect on  $r_h$ , as is usually found for block copoly(oxyalkylene)s.<sup>3,22,23</sup>

As noted in section 2.4, SLS intensities were usually measured at  $\theta = 90^\circ$ , as is appropriate for particles that are small relative to the wavelength of the light. For the present micellar solutions, the dissymmetries ( $I_{45}/I_{135}$ ) were 1.02 or less, which is consistent with micelles with small radii of gyration; a maximum value of  $r_g = 7$  nm can

**Table 3. Micelle Properties: ESE Copolymers in Aqueous Solution<sup>a</sup>**

copolymer	$T/^\circ\text{C}$	$N_w$	$r_h/\text{nm}$	copolymer	$T/^\circ\text{C}$	$N_w$	$r_h/\text{nm}$
$E_{76}S_5E_{76}$	25	6	6.2	$E_{66}S_{13}E_{66}$	25	21	8.1
	50	10	6.8		50	26	8.3
$E_{82}S_8E_{82}$	25	11	7.1	$E_{67}S_{15}E_{67}$	25	25	8.3
	50	16	7.1		50	30	8.8
$E_{82}S_9E_{82}$	25	14	7.8	$E_{112}S_9E_{112}$	25	8	7.7
	50	17	7.9		40	10	7.7
$E_{65}S_{11}E_{65}$	25	19	7.7	$E_{142}S_{19}E_{142}$	25	33	12.7
	50	22	7.8		50	35	12.1

<sup>a</sup> Estimated uncertainty in  $N_w$  and  $r_h$ :  $\pm 5\%$ .

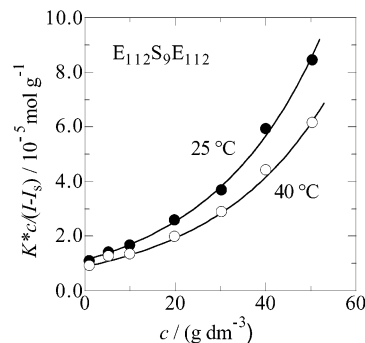


**Figure 6.** Debye plots for aqueous solutions of copolymer  $E_{112}S_9E_{112}$  at the temperatures indicated. The curves were calculated using theory for hard spheres.<sup>24</sup>

be estimated from  $r_g = 0.775r_h$  ( $r_h$  from Table 3) by treating the micelles as uniform spheres.

The Debye equation taken to the second term ( $A_2$  only) could not be used to analyze the SLS data, as micellar interaction caused curvature of the Debye plot across the concentration range investigated. This feature is illustrated in Figure 6, which shows Debye plots for solutions of copolymer  $E_{112}S_9E_{112}$  at 25 and 40 °C. In that figure the curves drawn through the data points are based on scattering theory for hard spheres.<sup>24</sup>

In the fitting procedure, the interparticle interference factor (structure factor,  $S$ ) in the scattering equation

$$K^*c/(I - I_0) = 1/SM_w \quad (8)$$

is approximated by

$$1/S = [(1 + 2\phi)^2 - \phi^2(4\phi - \phi^2)] (1 - \phi)^{-4} \quad (9)$$

where  $\phi$  is the volume fraction of equivalent uniform spheres. Values of  $\phi$  were calculated from the volume fraction of micelles in the system by applying a thermodynamic expansion factor  $\delta_t = v_i/v_a$ , where  $v_i$  is the thermodynamic volume of the micelles (i.e. one-eighth of the volume,  $u$ , excluded by one micelle to another) and  $v_a$  is the anhydrous volume of the micelles ( $v_a = M_w/N_A\rho_a$ , where  $N_A$  is Avogadro's constant and  $\rho_a$  is the liquid density of the copolymer solute calculated from published data assuming mass additivity of specific volumes).<sup>25,26</sup> The parameter  $\delta_t$  applies as an equivalent (effective) parameter for compact micelles irrespective of their exact structure. The method is equivalent to using the virial expansion for the structure factor of effective hard spheres taken to its seventh term but requires just two adjustable parameters, i.e.  $M_w$  and  $\delta_t$ .

(24) (a) Percus, J. K.; Yeivick, G. J. *J. Phys. Rev.* **1958**, *110*, 1. (b) Vrij, A. *J. Chem. Phys.* **1978**, *69*, 1742. (c) Carnahan, N. F.; Starling, K. E. *J. Chem. Phys.* **1969**, *51*, 635.

(25) Mai, S.-M.; Booth, C.; Nace, V. M. *Eur. Polym. J.* **1997**, *33*, 991.

(26) Kern, R. J. *Makromol. Chem.* **1965**, *81*, 261.

(23) Attwood, D.; Collett, J. H.; Tait, C. J. *Int. J. Pharm.* **1985**, *26*, 25.

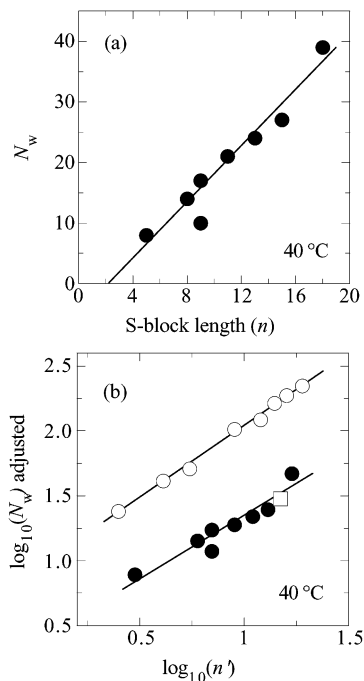


**Figure 7.** (a) Dependence of association number on S-block length for ESE triblock copolymers. (b)  $\log(N_w)$  versus  $\log(n')$  ( $n' = n - n_{cr}$ ) for (●) ESE triblock copolymers, (○) ES diblock copolymers (ref 7, 8, and 10), and copolymer (□)  $E_{205}St_{17}E_{205}$  (ref 12c). The results for the diblock copolymers are adjusted to a common length  $m = 50$  and those for the triblock copolymers to a common length  $m = 80$ .

Representative values of the derived association numbers ( $N_w = M_w/M_{w,mol}$ , with  $M_{w,mol}$  taken from Table 1) are listed in Table 3. The value of  $N_w$  for a given copolymer increases as temperature is increased, as would be expected, since water becomes a poorer solvent for the unimers as temperature is increased. This is consistent with the effect of temperature on micelles of many other copoly(oxyalkylene)s.<sup>3,22</sup> Considered at constant temperature,  $N_w$  increases with hydrophobe block length. This effect is illustrated in Figure 7a by the plot of  $N_w$  against S-block length for the triblock copolymers in solution at 40 °C. The intercept with the abscissa defines the critical S-block length for micellization,  $n_{cr} \approx 2$ , which is twice that found for diblock ES copolymers,<sup>8</sup> i.e. consistent with results for diblock and triblock E/B copolymers.<sup>3</sup> The log–log plot shown in Figure 7b compares values of  $N_w$  for diblock and triblock copolymers, both in solution at 40 °C. In this figure the plot is against  $n' = (n - n_{cr})$ , with appropriate choice of  $n_{cr}$ . E-block length ( $m$ ) is an important determinant of  $N_w$ , and recent investigations<sup>3,27,28</sup> have yielded scaling exponents,  $N_w \sim m^a$  with  $a$  in the range  $-0.5$  to  $-0.6$ . Adopting the exponent used previously<sup>10</sup> for diblock ES copolymers, i.e.,  $N_w \sim m^{-0.5}$ , the data for the ES and ESE copolymers have been adjusted to  $m = 50$  for the diblocks (as in ref 10) and  $m = 80$  for the triblocks (a rough average of  $m$  for the eight copolymers investigated by light scattering).

In Figure 7b, the line through the data points for the diblock copolymers is of slope  $1.11 \pm 0.03$ , and that for the triblock copolymers is of slope  $0.97 \pm 0.13$ . Though qualified by the experimental error involved, these results favor the association numbers of the triblock copolymers

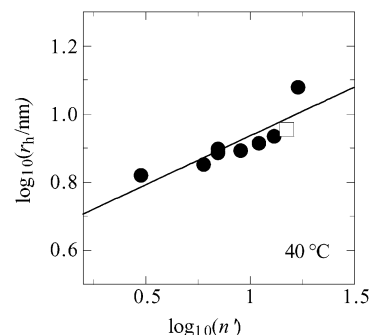


**Figure 8.** Dependence of hydrodynamic radius on S-block length.  $\log(r_h)$  versus  $\log(n')$  ( $n' = n - n_{cr}$ ) for (●) ESE triblock copolymers and (□)  $E_{205}St_{17}E_{205}$  (ref 12b).

being marginally less dependent on S-block length than those of comparable diblock copolymers. A similar log–log plot of hydrodynamic radius against  $n'$  (see Figure 8), but uncorrected for variation in E-block length, has a slope of  $0.29 \pm 0.06$ , also marginally lower than that obtained for diblock ES copolymers ( $0.34 \pm 0.05$ ).<sup>10</sup>

Very few values of association numbers and radii have been reported for  $E_mSt_nE_m$  copolymers with  $n < 20$ . Hydrodynamic radii reported by Bahadur and Sastry<sup>11</sup> for copolymers  $E_{68}St_{13}E_{68}$ ,  $E_{38}St_{15}E_{38}$ , and  $E_{77}St_{15}E_{68}$  (our notation) are in the range 4.5–2.5 nm, i.e., much smaller than the values found in this work (Table 3) for comparable copolymers and, indeed, much smaller than would be expected by comparison with results for other triblock copolymers.<sup>3,22</sup> Unfortunately, details of the collection and analysis of their DLS data are not given in ref 11. Values of  $N_w = 19$  and  $r_h = 9$  nm reported by Winnik and co-workers<sup>12b,c</sup> for copolymer  $E_{205}St_{17}E_{205}$  are similar to our results: see Figures 7 and 8. In Figure 7, the value  $N_w = 19$  has been scaled by  $m^{-0.5}$  to a value consistent with  $m = 80$  to obtain  $N_w = 30$ .

**3.4. Gel Diagrams and Gel Properties.** Tube inversion was used to define the immobile gel regions of the gel–sol diagrams. Immobility in the test described in section 2.5 requires the gel to have a yield stress  $\sigma_y \geq 30$  Pa.<sup>29,30</sup> For spherical micelles packed in a cubic array, it is known that  $\sigma_y/G \approx 0.1$  with  $G$  measured at 1 Hz, which means a storage modulus for cubic hard gel of  $G \geq 1$  kPa.<sup>29,30</sup> Such a gel is referred to by Hvidt et al. as a “hard gel”.<sup>31,32</sup> Figure 9 illustrates the hard gel regions observed for a number of the triblock copolymers. Mobile–immobile transitions on heating, which are usually found for solutions of other block copoly(oxyalkylene)s,<sup>33</sup> were not observed. A feature of the results is an increase in the high-temperature stability of the hard gels with increase in S-block length. This is similar to the effect reported for diblock copolymers with S-block lengths from  $S_5$  to  $S_{20}$ ,<sup>7,8,10</sup> and also for  $E_mB_n$  diblock copolymers.<sup>30</sup>

Recent studies<sup>34</sup> by small-angle X-ray scattering (SAXS) of 30 wt % gels at 25 °C of several of the present copolymers have shown them to comprise spherical micelles packed

(29) Kellarakis, A.; Mingvanish, W.; Daniel, C.; Li, H.; Havredaki, V.; Heatley, F.; Booth, C.; Hamley, I. W.; Ryan, A. J. *Phys. Chem. Chem. Phys.* **2000**, *2*, 2755.

(30) Mingvanish, W.; Kellarakis, A.; Mai, S.-M.; Daniel, C.; Yang, Z.; Havredaki, V.; Hamley, I. W.; Ryan, A. J.; Booth, C. *J. Phys. Chem. B* **2000**, *104*, 9788.

(31) Hvidt, S.; Jørgensen, E. B.; Brown, W.; Schillén, K. *J. Phys. Chem.* **1994**, *98*, 12320.

(32) Almgren, M.; Brown, W.; Hvidt, S. *Colloid Polym. Sci.* **1995**, *273*, 2.

(33) Hamley, I. W.; Mai, S.-M.; Ryan, A. J.; Fairclough, J. P. A.; Booth, C. *Phys. Chem. Chem. Phys.* **2001**, *3*, 2972.

(34) Castelletto, V.; Hamley, I. W.; Crothers, M.; Attwood, D.; Yang, Z.; Booth, C. *Macromol. Sci. Phys.* Submitted

(27) Kellarakis, A.; Havredaki, V.; Viras, K.; Mingvanish, W.; Heatley, F.; Booth, C.; Mai, S.-M. *J. Phys. Chem. B* **2001**, *105*, 7384.

(28) Chaibundit, C.; Mai, S.-M.; Heatley, F.; Booth, C. *Langmuir* **2000**, *16*, 9645.

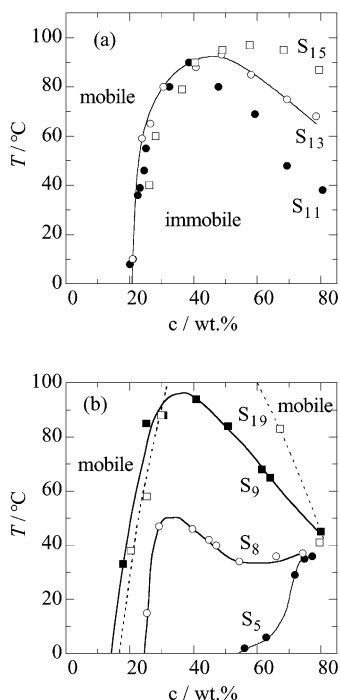


**Figure 9.** Phase diagrams from tube inversion showing immobile (gel) and mobile regions. (a) Aqueous solutions of copolymers (●)  $E_{65}S_{11}E_{65}$ , (○)  $E_{66}S_{13}E_{66}$ , and (□)  $E_{67}S_{15}E_{67}$ . (b) Aqueous solutions of copolymers (●)  $E_{76}S_5E_{76}$ , (○)  $E_{82}S_8E_{82}$ , (■)  $E_{82}S_9E_{82}$ , and (□)  $E_{142}S_{19}E_{142}$ . Low-temperature boundaries to the gel phases were not observed.

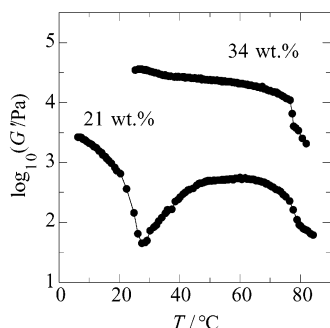


**Figure 10.** Temperature dependence of  $\log(G')$  (●) for aqueous hard gels of copolymer  $E_{66}S_{13}E_{66}$  at the concentrations indicated. Frequency = 1 Hz, strain amplitude  $\leq 0.6\%$ .

in cubic arrays, usually in body-centered structures. In corresponding aqueous gels of related diblock copolymers ( $S_{13}E_{60}$ ,  $S_{15}E_{63}$ ,  $S_{17}E_{65}$ ,  $S_{20}E_{67}$ ), the micelles are more usually packed in face-centered cubic structures.<sup>34,35</sup> Micelle association numbers are smaller for the triblock copolymers ( $N_w < 40$  compared with  $N_w > 100$  for the diblocks), and their intermicellar potentials will be softer on this account, because of the lower density of E blocks in the micelle corona. A soft intermicellar potential is known to favor a bcc structure.<sup>33,36</sup>

Only solutions of copolymers  $E_{66}S_{13}E_{66}$  and  $E_{142}S_{19}E_{142}$  were investigated using the Bohlin rheometer. Examples of temperature scans of  $G'$  for solutions of copolymer  $E_{66}S_{13}E_{66}$  at concentrations above the minimum value for hard gel formation are shown in Figure 10. For both solutions,  $G' > G''$  over the temperature range of the gel. On the basis of a critical value of  $G' = 1$  kPa for a hard

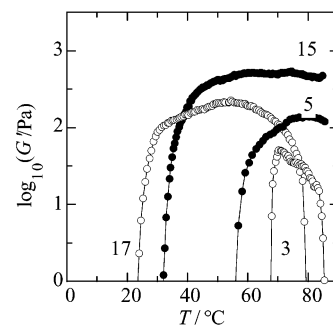


**Figure 11.** Temperature dependence of  $\log(G')$  for aqueous solutions of copolymers (○)  $E_{66}S_{13}E_{66}$  and (●)  $E_{142}S_{19}E_{142}$  at concentrations below the hard-gel boundary. Concentrations in wt % are indicated. Frequency = 1 Hz, strain amplitude  $\leq 0.6\%$ .

gel, the 21 wt % solution is a hard gel up to  $T \approx 20$  °C and a soft gel thereafter, and the 34 wt % solution is a hard gel up to 83 °C, with  $G' \approx 35$  kPa at 25 °C, the temperature used in the recent SAXS experiments.<sup>34</sup> The solutions in the temperature range of the soft gel were mobile in the tube-inversion test, but a storage moduli (measured at 1 Hz) significantly above the level characteristic of a sol (i.e.  $G' > 10$  Pa) with  $G' > G''$  means that they can be classified as “soft” gels.<sup>31,33</sup> Within the accuracy of determination,  $\pm 2$  °C, the hard gel boundaries from rheology and tube inversion were the same.

Examples of temperature scans of  $G'$  for solutions of copolymers  $E_{66}S_{13}E_{66}$  and  $E_{142}S_{19}E_{142}$  at concentrations below the hard-gel boundary are shown in Figure 11. Using the conditions described above, at temperatures at which  $G'$  (1 Hz) exceeds 10 Pa, the solutions are soft gels, otherwise sols. The maximum value of the storage modulus of the soft gel increases with increase in copolymer concentration, for example, from  $G' \approx 50$  Pa (3 wt %) to  $G' > 200$  Pa (17 wt %) for solutions of copolymer  $E_{66}S_{13}E_{66}$  (see Figure 11). The upper limit to the soft gel, observed for solutions of copolymer  $E_{66}S_{13}E_{66}$ , is not reached for copolymer  $E_{142}S_{19}E_{142}$  within the temperature range investigated,  $T < 90$  °C. This is consistent with the stability at high temperature of the hard gels of copolymer  $E_{142}S_{19}E_{142}$ .

The relation of the regions of sol and soft gel to hard gel is shown in Figure 12a for copolymer  $E_{66}S_{13}E_{66}$  and in Figure 12b for copolymer  $E_{142}S_{19}E_{142}$ . In Figure 12a, the two data points shown by filled triangles were obtained by rheometry as discussed above (Figure 10). Except that the upper temperature for soft gel formation is attained for solutions of copolymer  $E_{66}S_{13}E_{66}$ , the soft gel regions are similar for the two systems. In each case, the temperature of first formation of soft gel on heating falls with increase in concentration. The scatter in the points probably originates in the dependence of the soft gel boundary on shear/strain history, as discussed previously for related systems.<sup>29,37</sup>

The sol–gel diagrams in Figure 12 follow the same overall pattern as those published previously for diblock copolymers  $S_{13}E_{60}$  and  $E_{45}S_{10}$ <sup>8,10</sup> and for other diblock and triblock copoly(oxyalkylene)s.<sup>3,27,29,37,38</sup> The nature of soft gel has been discussed previously, and the present results do not change the picture.<sup>3</sup> In brief, a soft gel in concentrated solution (as illustrated in Figure 10) can be assigned as a defective cubic phase, while one in dilute solution (as illustrated in Figure 11) is thought to be a structure of weakly interacting spherical micelles formed

(35) Castelletto, V.; Hamley, I. W.; Holmquist, P.; Rekasas, C. J.; Booth, C.; Grossmann, J. G. *Colloid Polym. Sci.* **2001**, *279*, 621.

(36) Hamley, I. W.; Daniel, C.; Mingvanish, W.; Mai, S.-M.; Booth, C.; Messe, L.; Ryan, A. J. *Langmuir* **2000**, *16*, 2508.

(37) Li, H.; Yu, G.-E.; Price, C.; Booth, C.; Hecht, E.; Hoffmann, H. *Macromolecules* **1997**, *30*, 1347.

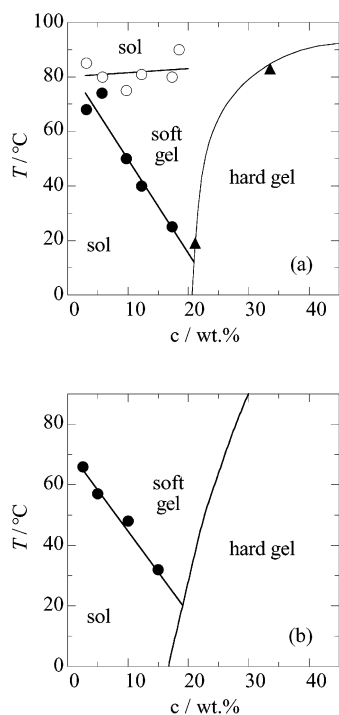


**Figure 12.** (a) Sol–gel diagram for aqueous solutions of triblock copolymer  $E_{66}S_{13}E_{66}$  showing the hard-gel boundary determined by tube inversion taken from Figure 9 and data points defined by rheometry on (▲) the hard-gel boundary, (●) the sol/soft-gel boundary, and (○) the soft-gel/sol boundary. (b) Corresponding phase diagram for triblock copolymer  $E_{142}S_{19}E_{142}$ . In this case the upper boundary of the soft gel was not attained.

from sol via a percolation transition. The assignment of dilute soft gels as percolation-induced structures differs from that made by Hvidt and co-workers for certain EPE

(38) Kellarakis, A.; Havredaki, V.; Booth, C. *Macromol. Chem. Phys.* accepted.

copolymers.<sup>31,32,39</sup> In those systems, a high-temperature soft gel is formed from cylindrical (rodlike) micelles, but we have no evidence for such micelles in our solutions.

#### 4. Concluding Remarks

Research on the properties of E/S copolymers in aqueous solution is at an early stage, and micellization behavior, micelle properties, and gelation require documentation. Indeed, this is the first paper to describe these properties for ESE triblock copolymers. The work is timely, as copolymers of this type have recently been introduced to the market. Our interest arises from the potential use of the micellar solutions of ES copolymers for solubilization of aromatic solutes. However, the flexibility introduced into the  $S_n$  chain by the ether link combined with the high hydrophobicity of the S unit suggest a broad field of application. The results discussed in this paper, and in a related report on diblock ES copolymers,<sup>10</sup> confirm features that are common with aqueous solutions of other block copoly(oxyalkylene)s and emphasize an important difference in gelation at low temperatures. Additionally, the combination of results for ES and EB copolymers provides a sufficiently wide range of hydrophobicity to reveal a significant transition in the dependence of the Gibbs energy of micellization on hydrophobe block length.

**Acknowledgment.** Mr. S. K. Nixon helped with the characterization of the copolymers. The project was supported by the Engineering and Physical Science Research Council (UK) through Grants GR/N63727 and GR/M96742, by the Erasmus Exchange Program of the European Union (A.K.), by the Ministry of Science and Technology, Spain, through project MAT2001-2877 (P.T. and V.M.), by the Brazilian Research Council CNPq (N.M.P.S.R.), by the Thai government (C.C.), and by GlaxoSmithKline (M.C.).

LA026479L

(39) Jørgensen, E. B.; Hvidt, S.; Brown, W.; Schillén, K. *Macromolecules* **1997**, *30*, 2355.